

Assessment of sowing dates and plant densities using CSM-CROPGRO-Soybean for soybean maturity groups in low latitude

L. S. Sampaio¹, R. Battisti² , M. A. Lana³  and K. J. Boote⁴

¹Universidade Federal Rural da Amazônia, Instituto de Ciências Agrárias, Belém, PA, Brazil; ²Universidade Federal de Goiás, Escola de Agronomia, Goiânia, GO, Brazil; ³Department of Crop Production Ecology, Swedish University of Agricultural Sciences, Uppsala, Sweden and ⁴Agricultural and Biological Engineering Department, University of Florida, Gainesville, FL, USA

Crops and Soils Research Paper

Cite this article: Sampaio LS, Battisti R, Lana MA, Boote KJ (2020). Assessment of sowing dates and plant densities using CSM-CROPGRO-Soybean for soybean maturity groups in low latitude. *The Journal of Agricultural Science* **158**, 819–832. <https://doi.org/10.1017/S0021859621000204>

Received: 9 September 2020

Revised: 9 February 2021

Accepted: 1 March 2021

First published online: 5 April 2021

Key words:

Crop management; crop modelling; *Glycine max* L; late maturity group; potential yield

Author for correspondence:

R. Battisti, E-mail: battisti@ufg.br

Abstract

Crop models can be used to explain yield variations associated with management practices, environment and genotype. This study aimed to assess the effect of plant densities using CSM-CROPGRO-Soybean for low latitudes. The crop model was calibrated and evaluated using data from field experiments, including plant densities (10, 20, 30 and 40 plants per m²), maturity groups (MG 7.7 and 8.8) and sowing dates (calibration: 06 Jan., 19 Jan., 16 Feb. 2018; and evaluation: 19 Jan. 2019). The model simulated phenology with a bias lower than 2 days for calibration and 7 days for evaluation. Relative root mean square error for the maximum leaf area index varied from 12.2 to 31.3%; while that for grain yield varied between 3 and 32%. The calibrated model was used to simulate different management scenarios across six sites located in the low latitude, considering 33 growing seasons. Simulations showed a higher yield for 40 pl per m², as expected, but with greater yield gain increments occurring at low plant density going from 10 to 20 pl per m². In Santarém, Brazil, MG 8.8 sown on 21 Feb. had a median yield of 2658, 3197, 3442 and 3583 kg/ha, respectively, for 10, 20, 30 and 40 pl per m², resulting in a relative increase of 20, 8 and 4% for each additional 10 pl per m². Overall, the crop model had adequate performance, indicating a minimum recommended plant density of 20 pl per m², while sowing dates and maturity groups showed different yield level and pattern across sites in function of the local climate.

Introduction

Brazil was responsible for 34% of global soybean production in the 2018 growing season (FAOSTAT, 2020). The production occurred predominantly in the South and Midwestern Brazil, reaching 86% of total national production. Currently, North/Northeast Brazil is a new expansion area for soybean production. The region produced 14% of national production in the 2018/19 growing season (CONAB, 2020). This region is located in low latitude, from 10° south to 5° north. The expansion in this region has been made possible with the development of cultivars adapted to low latitude (<15°S), improved soil fertility and reduction of soil acidity (Cattelan and Dall'Agnol, 2018). In this scenario, the expansion of production area and increase of yield are important to supply global demand for food.

Soybean crop management for new regions has been based on the management for current production areas, which can lead to low efficiency to explore new environmental conditions, for example, using sowing dates, plant density and cultivars from other production regions that limit potential yield (Teixeira *et al.*, 2019). The management needs to be adapted for different environmental conditions to reduce risks associated with climate and production costs (Battisti *et al.*, 2020a) and to increase crop resilience (Halsnaes and Taerup, 2009). Crop management practices that can be used in new environments to improve yield and crop resilience, include sowing dates (Hu and Wiatrak, 2012; Spehar *et al.*, 2015), maturity group (Battisti *et al.*, 2018; Teixeira *et al.*, 2019) and irrigation (Justino *et al.*, 2019; Battisti *et al.*, 2020b).

In this context, plant density is a crop management practice with potential adaptation when considered the interaction between weather (air temperature, rainfall and photoperiod), soil (soil water availability to the crop) and other crop management (sowing date and maturity group) (Salmerón *et al.*, 2015, 2017). This combination can define potential yield for soybean (Van Roekel *et al.*, 2015). In Southern Brazil, Corassa *et al.* (2018) evaluated 109 replicated field trials with seeding rates of 10, 23, 30, 36 and 49 pl per m², with 2–12 genotypes (maturity groups from 4.2 to 6.3) per site. Corassa *et al.* (2018) concluded that plant density can be reduced up to 18% for fields with high yield potential (>5000 kg/ha) without losing yield when compared with fields of lower yield potential (<4000 kg/ha).

In northern Brazil, farmers have opted for early sowing dates with lower maturity groups (6.0–7.0) than recommended for the region (8.0–9.0) to get a short cycle which allows sowing

a second crop (maize off-season) in the same growing season (Nóia Júnior and Sentelhas, 2019; Battisti *et al.*, 2020a). A short cycle crop results in a recommendation to sow higher plant density to increase leaf area index (LAI) for optimal value (Lee *et al.*, 2008; Tagliapietra *et al.*, 2018). However, because of high seed costs farmers sow less seed than ideal, leading to yield losses. The yield losses can be avoided, by defining the best plant density for each combination of sowing date and maturity group for this environment. For that reason, mechanistic crop models can help to make better decisions based on probabilistic level considering climate, maturity groups, sowing dates and plant density (Boote *et al.*, 2013; Ewert *et al.*, 2015; Hooogenboom *et al.*, 2019).

The use of crop models requires evaluation of whether model responses are acceptable for the intended management (Nendel *et al.*, 2011). Studies have evaluated and used soybean crop models for plant density management (e.g. Basso *et al.*, 2001; Banterng *et al.*, 2009; Setiyono *et al.*, 2010; Battisti *et al.*, 2018). But, to the extent of our knowledge, there are no studies of simulated plant density response for production systems in low latitude (northern Brazil) using high maturity groups. In this context, this research hypothesizes that CSM-CROPGRO-Soybean is able to simulate development and growth after calibration, and can be used to define the best strategies considering the interaction of plant density, sowing dates and maturity group for the sites of low latitude in Brazil. Thus, our study aimed: (1) to calibrate and evaluate CSM-CROPGRO-Soybean regarding plant development, growth and yield in response to plant density for two soybean maturity groups (7.7 and 8.8); and (2) to assess the best crop management strategies (sowing dates \times plant densities \times maturity groups) based on seasonal analysis using long-term historical weather for six sites in low latitude.

Materials and methods

Data set for crop model calibration and evaluation

Field experiment description

The field experiments were conducted in Paragominas, Pará State, Brazil (Lat: -3.37° , Long: -47.42° , 176 m a.s.l.) (Fig. 1). The climate is classified as Aw according to Köppen climate classification, characterized by wet summers and a defined dry winter season (Alvares *et al.*, 2013) (Supplementary material, Fig. S1). On-farm field experiments were carried out in 2018 and 2019 under no-tillage using randomized block design with four replication, including three factors: two soybean cultivars, four plant densities and three sowing dates for crop model calibration, and two soybean cultivars, four plant density and one sowing date for crop model evaluation (Table 1). The cultivars were M7739 IPRO (maturity group 7.7 with semi-indeterminate growth habit), named hereafter as MG 7.7, and M8808 IPRO (maturity group 8.8, determinate growth habit), named hereafter as MG 8.8. Intended plant densities were 10, 20, 30 and 40 pl per m^2 , where results were discarded if the plant density was not reached (Table 1). The sowing dates were 06 Jan., 19 Jan. and 16 Feb. for the 2018 growing season, used for crop model calibration; and 12 Jan. for the 2019 growing season, used for crop model evaluation (Table 1). The plot size had 12 sowing rows (50-cm spacing between rows) with a length of 25 m, with a useful area of six rows by 3 m length delineated randomly inside the plot.

Crop management was done according to the farm schedule, including seed treatment with insecticide and fungicide, followed by biological inoculant containing strains of *Bradyrhizobium*:

SEMIA 5019 (*B. elkanii*) and SEMIA 5079 (*B. japonicum*) at an amount of 0.03 litres per ha. The soil fertilization was incorporated during sowing using 90 kg/ha of monoammonium phosphate (NPK: 12-61-0). Copper, cobalt and molybdenum were supplemented by foliar application. Weeds were controlled after sowing using glyphosate; pests were controlled by monitoring their presence every 5 days and diseases were controlled preventively, considering the action time of different chemical products; where these controls were aimed to avoid the presence of limiting factors.

Soil data collection

Soil chemical and physical attributes were sampled before sowing the field experiment at layers of 0–10, 10–20, 20–30, 30–50 and 50–70 cm depths. Four undisturbed samples were collected at the field using the volumetric ring to quantify soil water content at the soil saturation (SAT), at the drained upper limit (DUL), at the lower limit (LL) of plant extractable soil water, soil bulk density (BD) and hydraulic conductivity at saturation (KSAT) (Table 2), and three disturbed subsamples to quantify chemical and texture soil properties (Table 2). The DUL and LL points were quantified using the pressure plate method, respectively, at 10 and 1500 kPa. The initial soil water content was set at 50% of the difference between DUL and LL with the simulation initiated 30 days prior to the sowing date in the crop model.

Weather data collection

Daily weather data were obtained from an automatic weather station located at the experimental field, including maximum and minimum air temperature, total daily solar radiation and rainfall (Fig. 2). The mean (min–max) air temperatures were 26.4°C (18.9–38.8) and 27.0°C (19.8–37.3) respectively, for 2017/18 and 2018/19 growing seasons. The accumulated rainfalls were 1749 and 1928 mm from December to June, respectively, for 2017/18 and 2018/19 growing seasons. Total daily solar radiation had an average (min–max) of 18.2 (8.4–25.0) and 19.2 (6.5–28.6) MJ/ m^2 /day, respectively, for 2017/18 and 2018/19 growing seasons. The climatology for the field experiment site (Paragominas) is shown in Fig. S1 of the Supplementary material.

Measurements

The phenological stages were monitored weekly, recording the date when at least 50% of plot plants achieved the phenological characteristics described by Boote *et al.* (2003). The phenological stages were sowing, emergence (VE, cotyledons above soil surface), first flower (R1, when one open flower appeared on any node on the main stem), first seed (R5, when 3 mm seeds appeared on any node on the main stem) and beginning maturity (R7, when one pod with mature colour appeared on any node on the main stem). Total above-ground biomass, stem, leaf, pod, grain, LAI and leaf number were measured from three to six times during the growing season by sampling 1 linear metre of a row (0.5 m^2) from four replications. The samples occurred around 15, 30, 60, 75 and 90 days after sowing and at harvest for most of the treatments. Maturity group 7.7 did not have samples at 90 days after sowing, while for sowing dates on 16 Feb. 2018 and 12 Jan. 2019, the samples were done only at 40 and 75 days after sowing and at harvest.

The dry biomass was obtained after partitioning the plant in stem, leaf, pod and grain, drying at 70°C until constant weight. The LAI was determined by sampling leaves and scanning the whole leaf area with the LI-COR LI-3100C. The specific leaf

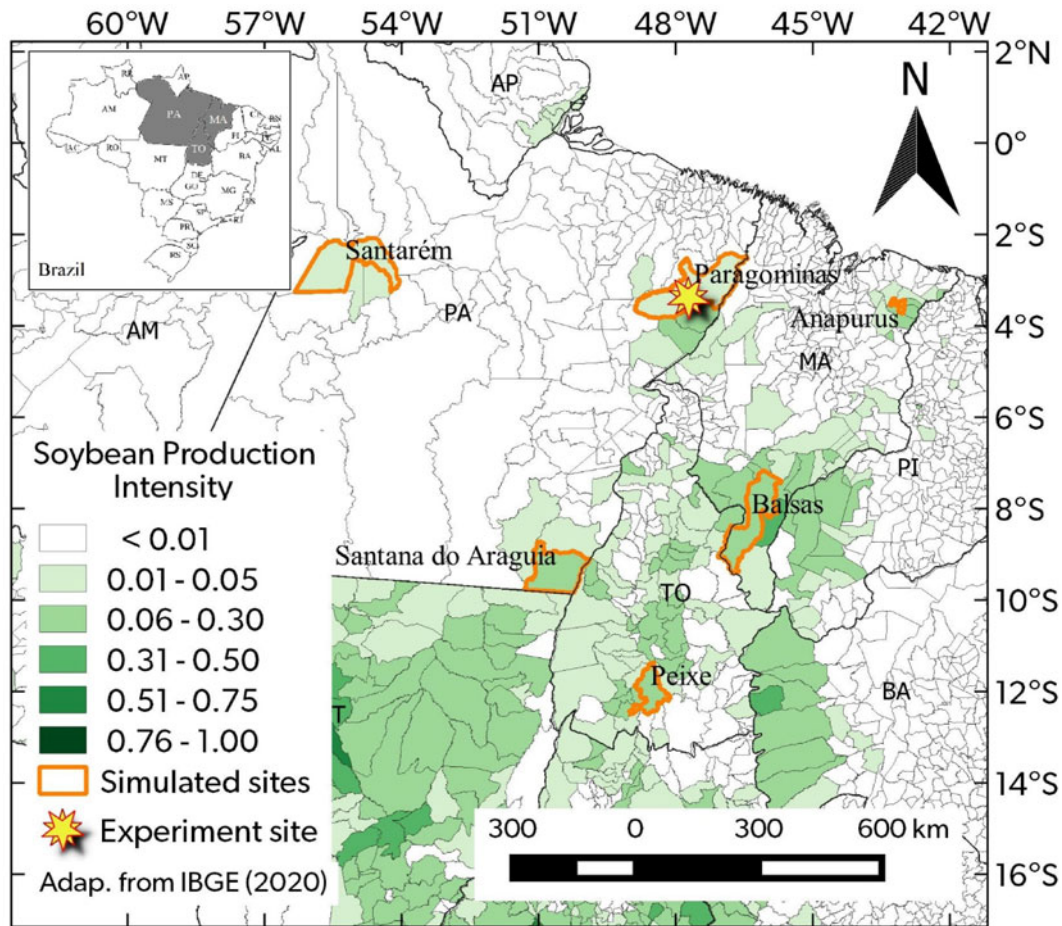


Fig. 1. (Colour online) State locations in Brazil (top left), experiment site, locations used for long-term yield simulation, soybean production intensity and municipality areas in the new expansion soybean area in Brazil. Adapted from IBGE (2020).

area was calculated by dividing leaf area (cm^2) by leaf biomass (g). Two central 1-m rows were harvested for final yield converted to dry mass, drying at 70°C until constant weight, and yield components (grain yield, number of pods, number of grains per pod and weight per grain). The harvest index was calculated by dividing grain yield by total aboveground biomass.

Crop model

Description of plant density response

The DSSAT CSM-CROPGRO-Soybean model v 4.7.0 (Hoogenboom *et al.*, 2017) is widely used in Brazil for management evaluation, for example, for tropical conditions (Banterng *et al.*, 2009), climate response (Silva *et al.*, 2017; Battisti and Sentelhas, 2019; Lima *et al.*, 2019) and irrigation (Battisti *et al.*, 2020b). The response to plant density is influenced by the LAI which affects crop evapotranspiration and photosynthesis rates during the life cycle. Leaf area growth depends on canopy photosynthesis, partitioning of biomass to leaf and the specific leaf area (response to temperature, light and water deficit) (Boote and Pickering, 1994; Boote *et al.*, 1998). The model simulates leaf senescence as a function of water deficit and nitrogen mobilization, as well as under high LAI because lower leaves receive low solar radiation. Plant density can indirectly affect water available to the crop through root density, as daily assimilate is partitioned to root mass and root length density leading to change in how the soil is explored

and the availability of water to the crop (Boote *et al.*, 1998). The root distribution with the soil profile depth is defined by the soil root growth factor (SRGF) (Table 2), and the same root profile shape was used for all plant densities in our study. The SRGF was obtained from Battisti *et al.* (2017).

Calibration and evaluation

The initial set of cultivar parameters for calibration was the generic cultivar parameters for maturity groups 7.0 and 8.0 from ecotype and cultivar file in the DSSAT-CROPGRO-Soybean for MG 7.7 and MG 8.8, respectively. The first step involved calibration of phenological coefficients such as first flower appearance (EM-FL), first pod (FL-SH) (adjusted to fit the onset of pod growth), first seed (FL-SD) and beginning maturity (SD-PM) (Hunt and Boote, 1998), in combination with critical short day length (CSDL) and slope of the relative response of development to photoperiod (PPSEN). Adjustments using observations were done to reduce bias and the root mean square error (RMSE) (Wallach *et al.*, 2006), comparing measured and simulated values using scatter plots.

After phenology calibration, growth parameters were calibrated in the second step. These included the maximum leaf photosynthesis rate (LFMAX), defined at 30°C , 350 vpm of CO_2 and high light; specific leaf area of cultivar under standard growth conditions (SLAVR); maximum size of full leaf (three leaflets) (SIZLF); time between first flower (R1) and end of leaf expansion

Table 1. Field experiment treatment data sets by plant densities, sowing dates and maturity groups during 2018 and 2019 growing seasons used for calibration and evaluation

Sowing date	Plant density (PD)		Maturity group	
	Pl per m ²		7.7	8.8
Calibration				
06 Jan. 2018	10	X	X	
	20	X	X	
	30	X		Missing PD ^a
	40	X	X	
19 Jan. 2018	10	X	X	
	20	X	X	
	30	X		Missing PD
	40	Missing PD		Missing PD
16 Feb. 2018	10	Missing PD		X
	20	X		Missing PD
	30	X		Missing PD
	40	Missing PD		X
Evaluation				
12 Jan. 2019	10	X	X	
	20	X	X	
	30	X	X	
	40	X	X	

^aMissing PD means that the intended plant density was not reached, therefore results were discarded.

(FL-LF); maximum weight per seed (WTPSD); seed filling duration for pod cohort at standard growth conditions (SFDUR); average seed number per pod under standard growing conditions (SDPDV); time required for cultivar to reach final pod load under optimal conditions (PODUR) and threshing percentage between grain and pod (THRSH).

Growth parameters were adjusted simultaneously using generalized likelihood uncertainty analysis (GLUE) (Makowski *et al.*, 2002; Jones *et al.*, 2011) available within DSSAT to adjust LFMAX, SLAVR and SIZLF. The target of GLUE was only the final yield values. Therefore, subsequent manual calibration was done to improve the model performance against time-series growth analysis using scatter plots for yield, LAI and biomass partitioning, including bias and RMSE (Wallach *et al.*, 2006). The GLUE was set to run 15 000 simulations, following the recommendation of Jones *et al.* (2011). After the optimization with GLUE and the manual calibration, parameters were checked to verify their consistency with other calibrations and maturity group characteristics in the model database. After calibration, the crop model was evaluated with independent data measured in the 2019 growing season (Table 2).

Model application over multiple weather seasons at six sites

Crop management was simulated using DSSAT's Seasonal Analysis software considering sowing dates, plant densities and maturity groups for six sites in northern Brazil. The sites were: Paragominas, Santarém, Santana do Araguaia, Anapurus, Balsas

and Porto Nacional (Fig. 1). The daily weather data for 33 growing seasons were obtained from 01 Jan. 1980 to 31 Dec. 2013 (Xavier *et al.*, 2015). The climatology for these sites can be found in Fig. S1 of the Supplementary material. The simulated crop management included four plant densities of 10, 20, 30 and 40 pl per m²; two maturity groups (7.7 and 8.8); and sowing dates every 10 days during the sowing windows for each region (Table 3), defined based on agroclimatic zoning risk (MAPA, 2020). The soil type and texture by site were obtained from RADAM (1974) (Table 3), while the soil water characteristics were obtained from Battisti and Sentelhas (2019) (Supplementary material, Table S1). The Seasonal Analysis was initiated 3 months prior to each sowing date, assuming initial soil water content at 50% of the difference between DUL and LL, with initial conditions reinitiated every growing season.

Results

Crop model performance compared to experimental data

The parameters calibrated can be found in Table 4 for MG 7.7 and 8.8. In the calibration process, the first step was to adjust parameters of CSDL and PPSEN to improve the prediction of first flower occurrence, followed by calibrating EM-FL, FL-SH, FL-SD and SD-PM. Then FL-LF, SLAVR and SIZLF were modified to improve LAI simulation, where it was necessary to modify parameters to improve LAI mainly for the lower plant density. FL-LF was increased for MG 7.7 due to its indeterminate flowering habit (start flowering early and indeterminate leaf area growth), while FL-LF for MG 8.8 was not changed from the generic default determine cultivar parameters because of its determinate growth habit. LFMAX was adjusted to increase biomass production, as this parameter increases both LAI and biomass. The default LFMAX value of 1.03 was increased to 1.20 and 1.175 $\mu\text{mol}/\text{m}^2/\text{s}$, respectively, for MG 7.7 and 8.8. The final changes involved parameters related to pod and grain growth duration, to improve yield simulation (Table 4).

Phenology

For calibration, the model had a bias lower than 2 days for emergence, first flower, first seed and beginning maturity for MG 7.7 and 8.8 (Table 5), with a strong agreement between measured and simulated (Figs 3(a) and (b)). The evaluation was in agreement across crop stages for MG 7.7, with bias less than 1.3 days (Table 5) and strong agreement between measured and simulated (Fig. 3(a)). However, MG 8.8 showed a longer time to the occurrence of beginning maturity (bias = 7 days; Table 5); while anthesis occurred 4 days early in the crop model simulation (Table 5). There were no observed or simulated effects of plant density on crop phenology.

Time-series of leaf area index and biomass

LAI was simulated well across plant densities and sowing dates for MG 7.7 for both model calibration and evaluation processes (Fig. 4). For calibration, the RMSE was lower than 1.23 (relative RMSE (RRMSE) <33%; bias <1.08) (Supplementary material, Table S2). The later sowing dates (19 Jan. and 16 Feb.) showed a higher observed LAI than simulated, being higher during the middle to end of the cycle for 19 Jan. sowing (Fig. 4(b)), and a more rapid reduction for 16 Feb. (Fig. 4(c)). This performance

Table 2. Soil layer characteristics measured prior to planting in the field experiment in Paragominas, PA

Depth layer (cm)	pH (CaCl ₂)	OM (g/kg)	P _{resin} (mg/dm ³)	K (cmolc/dm ³)	Ca (cmolc/dm ³)	Mg (cmolc/dm ³)	H + Al (cmolc/dm ³)	CEC (cmolc/dm ³)	V (%)
0–10	5.3	20.4	20.6	0.22	3.10	1.30	3.00	7.62	60.6
10–20	5.0	14.8	15.7	0.21	2.67	0.96	1.30	7.04	54.5
20–30	4.7	9.5	10.6	0.19	2.08	0.72	0.96	5.69	52.5
30–50	4.7	6.7	9.6	0.15	1.78	0.52	0.72	6.45	38.1
50–70	4.7	3.5	6.6	0.11	1.04	0.36	0.52	5.01	30.2
70–300	4.7	3.5	6.6	0.11	1.04	0.36	0.52	5.01	30.2
Depth (cm)	Sand (%)	Silt (%)	Clay (%)	BD (g/cm ³)	KSAT (cm/h)	SAT (cm ³ /cm ³)	DUL (cm ³ /cm ³)	LL (cm ³ /cm ³)	
0–10	11	12	77	1.0	3.0	0.58	0.49	0.24	
10–20	7	13	80	1.2	3.0	0.52	0.42	0.27	
20–30	4	11	84	1.3	3.0	0.50	0.46	0.30	
30–50	4	12	84	1.3	1.0	0.49	0.43	0.31	
50–70	4	12	84	1.3	1.0	0.49	0.43	0.31	
70–300	4	12	84	1.3	1.0	0.49	0.43	0.31	
	Soil layer			SRGF	Soil layer			SRGF	
	1 (0–5 cm)			1	7 (60–70 cm)			0.18	
	2 (5–15 cm)			1	8 (70–100 cm)			0.16	
	3 (15–30 cm)			0.42	9 (100–125 cm)			0.04	
	4 (30–40 cm)			0.34	10 (125–150 cm)			0.04	
	5 (40–50 cm)			0.23	11 (150–160 cm)			0.00	
	6 (50–60 cm)			0.20	12 (160–300 cm)			0.00	

OM, organic matter; P_{resin}, phosphorus extracted by ion exchange resins; CEC, cation-exchange capacity; V, base-cation saturation ratio; BD, soil bulk density; KSAT, hydraulic conductivity at saturation; SAT, soil water content at soil saturation; DUL, soil water content at drained upper limit; LL, lower limit of plant extractable soil water. The layer 70–300 cm was obtained extrapolating the last measured layer (50–70 cm). SRGF, soil root growth factor, obtained from Battisti *et al.* (2017).

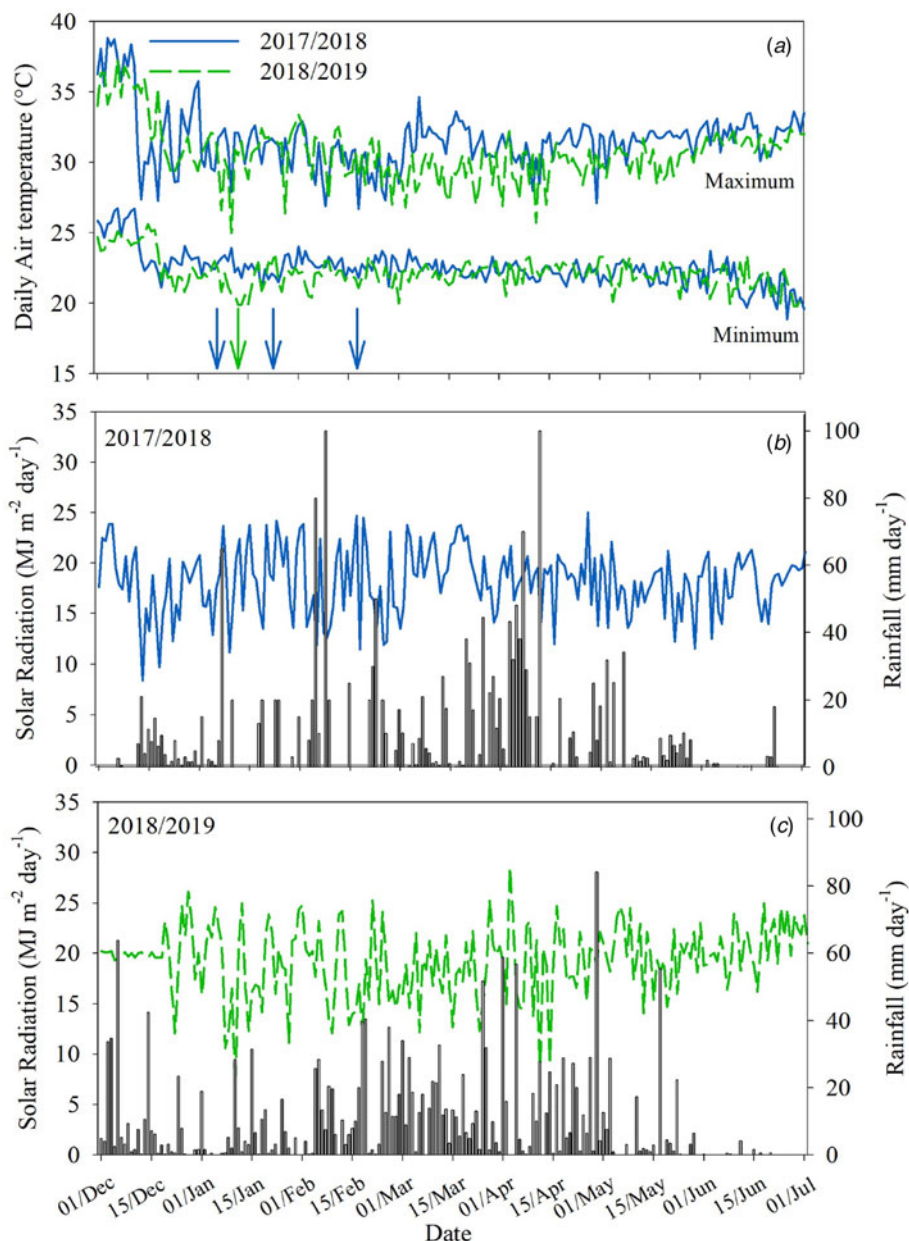


Fig. 2. (Colour online) Maximum and minimum air temperature (a), total daily solar radiation (b and c) and rainfall (b and c) for field experiment conducted during 2017/18 (a and b) and 2018/19 (a and c) growing seasons. In (a), the arrow indicates the sowing date for soybean and in (b) and (c), the continuous line is total daily solar radiation and bar graph is rainfall.

was similar during evaluation for the sowing on 12 Jan. for four plant densities, with the field experiment having higher LAI late in the cycle when compared with simulated (Fig. 4(d)), although the crop model simulated higher main stem leaf (node) number during the evaluation (bias = 0.71) (Table 5).

The simulated and observed LAI were similar during the growing cycle for MG 8.8. A limitation was that the model overpredicted LAI for high plant density, as can be observed for 40 pl per m² for sowing date on 06 Jan. (Fig. 4(e)) and 16 Feb. (Fig. 4(g)), where RRMSE was 28 and 19%, respectively (Supplementary material, Table S2). Simulated LAI was higher than observed for 10 pl per m², where RRMSE were between 5 and 13% (Supplementary material, Table S2). For the model evaluation, the RRMSE increased with higher plant densities. RRMSE was 5% for 10 pl per m², while it reached 32% at 40 pl per m² (Supplementary material, Table S2).

The model response to plant density was well predicted for biomass and the individual components of biomass across crop cycle (pod, leaf and stem). The fractional partitioning between pod, leaf and stem for MG 7.7 was not affected by plant densities (true of the data as well as the model) (Figs 5(a–d)). For model calibration, the aboveground dry biomass for MG 7.7 had RMSE lower than 975 kg/ha (RRMSE <26%) (Supplementary material, Table S3) for time-series data, while for end-of-season, including all plant density, the overall RMSE was 489 kg/ha (RRMSE = 11.4%) (Table 5). The results from model evaluation revealed that RMSE for aboveground dry biomass increased to 1220 kg/ha, but with RRMSE of 21% for time-series data, while overall performance at end-of-season showed RMSE of 268 kg/ha (RRMSE = 4.6%) (Table 5). The bias for leaf and pod dry mass were similar during calibration and evaluation, being between –395 and –17 kg/ha for leaf (Supplementary material, Table S4), and between –460 and 622 kg/ha for pod (Supplementary material, Table S5), showing agreement across

Table 3. Sites, geographic location, sowing window dates and soil type considered in the seasonal analyses for soybean management in the north Brazil

Sites	Lat ^a (°)	Long ^b (°)	Elev ^c (m)	Sowing dates ^d		Soil type ^e
				Start	End	
Paragominas, PA	-3.35	-47.37	90	01 Dec.	21 Feb.	Clayey
Santarém, PA	-2.54	-55.34	35	01 Dec.	21 Feb.	Clayey
Santana do Araguaia, PA	-9.49	-50.52	160	01 Oct.	21 Dec.	Sandy-clay
Anapurus, MA	-3.62	-43.08	68	01 Dec.	21 Feb.	Sandy-clay
Balsas, MA	-7.55	-46.59	283	01 Oct.	21 Jan.	Sandy-clay
Porto Nacional, TO	-10.57	-48.49	212	01 Oct.	21 Dec.	Sandy-clay

^aLat is the latitude.^bLong is the longitude.^cElev is the elevation (m above sea level).^dSowing was done every 10 days.^eSoil parameters are shown in Table S1 of the Supplementary material.**Table 4.** Calibrated soybean cultivar parameters for the MG 7.7 and 8.8 in the CSM-CROPGRO-Soybean crop model

Traits ^a	Description	Values	
		MG 7.7	MG 8.8
#ECO	Code for the ecotype to which this cultivar belongs	SB0701	SB0801
CSDL	Critical short day length below which reproductive development progresses with no daylength effect (for short day plants) (h)	11.80	11.50
PPSEN	Slope of the relative response of development to photoperiod with time (positive for short day plants) (1/h)	0.325	0.340
EM-FL	Time between plant emergence and flower appearance (R1) (photothermal days)	25.00	24.50
FL-SH	Time between first flower and first pod (R3) (photothermal days)	5.00	8.20
FL-SD	Time between first flower and first seed (R5) (photothermal days)	10.50	12.00
SD-PM	Time between first seed (R5) and physiological maturity (R7) (photothermal days)	27.50	25.00
FL-LF	Time between first flower (R1) and end of leaf expansion (photothermal days)	22.00	18.00
LFMAX	Maximum leaf photosynthesis rate at 30°C, 350 vpm CO ₂ and high light (mg CO ₂ /m ² s)	1.200	1.175
SLAVR	Specific leaf area of cultivar under standard growth conditions (cm ² /g)	365	388
SIZLF	Maximum size of full leaf (three leaflets) (cm ²)	230	216
XFRT	Maximum fraction of daily growth that is partitioned to seed + shell	1.00	1.00
WTPSD	Maximum weight per seed (g)	0.15	0.16
SFDUR	Seed filling duration for pod cohort at standard growth conditions (photothermal days)	18.2	25.0
SDPDV	Average seed per pod under standard growing conditions (#/pod)	2.0	2.06
PODUR	Time required for cultivar to reach final pod load under optimal conditions (photothermal days)	10.0	10.0
THRSH	The maximum ratio of (seed/(seed + shell)) at maturity. Causes seed to stop growing as their dry weights increase until shells are filled in a cohort (threshing percentage)	76.0	78.0
SDPRO	Fraction protein in seeds (g(protein)/g(seed))	0.40	0.40
SDLIP	Fraction oil in seeds (g(oil)/g(seed))	0.20	0.20
V1-JU ^b	Time required from first true leaf to end of the juvenile phase, thermal days	6.00	6.00

^aTraits are described in Boote *et al.* (2003).^bV1-JU is in the ecotype file.

crop cycle (Fig. 5). The LAI and leaf dry biomass resulted in a good simulation of specific leaf area for most of the plant densities (RRMSE between 2 and 40%), but with high RRMSE for low plant densities and early planting dates (Supplementary material, Table S7).

The aboveground dry biomass was overpredicted by the model in the last date of measurement for MG 8.8 in the calibration and evaluation (Figs 5(e-h)). As expected, the RMSE aboveground dry biomass was larger for 40 than for 10 pl per m² (increasing from 499 to 652 kg/ha in calibration and from 798 to 1206 kg/ha in

Table 5. Measured (M), simulated (S), bias, RMSE and RRMSE (%) for crop end -season variables simulated by crop model in the calibration and evaluation steps for maturity groups (MG) 7.7 and 8.8

Variables	Calibration					Evaluation				
	M	S	Bias	RMSE	RRMSE	M	S	Bias	RMSE	RRMSE
	MG 7.7									
Emergence day	4.50	5.50	1.00	–	–	4.00	5.00	1.00	–	–
Anthesis day	34.75	35.00	0.25	–	–	35.00	35.00	0.00	–	–
1st seed day	48.00	49.75	1.75	–	–	52.00	50.00	–2.00	–	–
Maturity day	85.00	86.25	1.25	–	–	85.00	87.00	2.00	–	–
Canopy height (m)	0.55	0.68	0.13	0.15	27	0.52	0.69	0.17	0.18	35
Maximum LAI	4.03	3.51	–0.52	0.71	18	4.25	3.79	–0.46	0.52	12
Leaf number on main stem	11.19	11.34	0.14	0.44	4	10.64	11.35	0.71	0.74	7
Grain number per m ²	2107	2043	–64	176	8	2150	2017	–133	154	7
Grain number per pod	2.01	2.00	–0.01	0.11	5	1.81	2.00	0.19	0.20	11
Grain weight (g/unit)	0.16	0.17	0.01	0.01	6	0.16	0.17	0.01	0.01	6
Tops weight (kg/ha)	5402	5620	218	583	11	5757	5798	41	268	5
Pod weight (kg/ha)	4298	4452	154	489	11	4370	4497	127	227	5
Grain yield (kg/ha)	3339	3427	88	401	12	3453	3475	21	119	3
	MG 8.8									
Emergence day	4.57	5.43	0.86	–	–	4.00	5.00	1.00	–	–
Anthesis day	38.14	36.86	–1.29	–	–	41.00	37.00	–4.00	–	–
1st seed day	57.86	57.57	–0.29	–	–	57.00	58.00	1.00	–	–
Maturity day	95.57	96.00	0.43	–	–	91.00	98.00	7.00	–	–
Canopy height (m)	0.57	0.77	0.20	0.21	37	0.67	0.78	0.11	0.13	19
Maximum LAI	4.07	4.22	0.15	0.60	15	3.80	4.82	1.02	1.19	31
Leaf number on main stem	13.63	12.74	–0.89	1.10	8	13.47	12.72	–0.75	0.83	6
Grain number per m ²	2693	2528	–165	488	18	2228	2712	484	505	23
Grain number per pod	2.18	2.06	–0.12	0.14	6	1.99	2.06	0.07	0.11	6
Grain weight (g/unit)	0.14	0.15	0.01	0.02	14	0.14	0.15	0.01	0.01	7
Tops weight (kg/ha)	6303	6939	636	811	13	6029	7511	1482	1497	25
Pod weight (kg/ha)	4877	5091	214	524	11	4291	5686	1395	1442	34
Grain yield (kg/ha)	3729	3704	–24	384	10	3203	4189	986	1035	32

evaluation) (Supplementary material, Table S3). The model simulated well the values and the dynamics of aboveground dry biomass (Figs 5(e–h)), with RRMSE ranged from 7 and 16% for calibration, and 21 to 28% for evaluation (Supplementary material, Table S3). The leaf dry mass had low RRMSE during calibration (between 13 and 22%) (Supplementary material, Table S4) than during evaluation, when RRMSE increased from 10 to 33% with plant densities, respectively, from 10 to 40 pl per m² (Supplementary material, Table S4); although specific leaf area had a similar RRMSE, from 7 to 27% during calibration, and from 11 to 21 during evaluation (Supplementary material, Table S7).

Grain yield

Grain yield had an RMSE and RRMSE, respectively, of 401 kg/ha and 12% for calibration, and 119 kg/ha and 3% for evaluation for

MG 7.7 (Fig. 6(a)). The biases were 88 and 21 kg/ha, respectively, for calibration and evaluation (Table 5). MG 8.8 had similar performance for calibration to MG 7.7, resulting in a RMSE and RRMSE, respectively, of 384 kg/ha and 10% (Fig. 6(b)), with a bias of –24 kg/ha (Table 5). However, RRMSE was larger for evaluation of MG 8.8, with 32% (RMSE = 1035 kg/ha) and a bias of 986 kg/ha (Fig. 6(b)). In this case, the model showed a yield response higher than field experiments across plant densities.

Seasonal analysis application: sowing dates × plant density × cultivars

Seasonal analysis over 33 seasons showed that higher plant density (40 pl per m²) resulted in higher yield than lower plant density

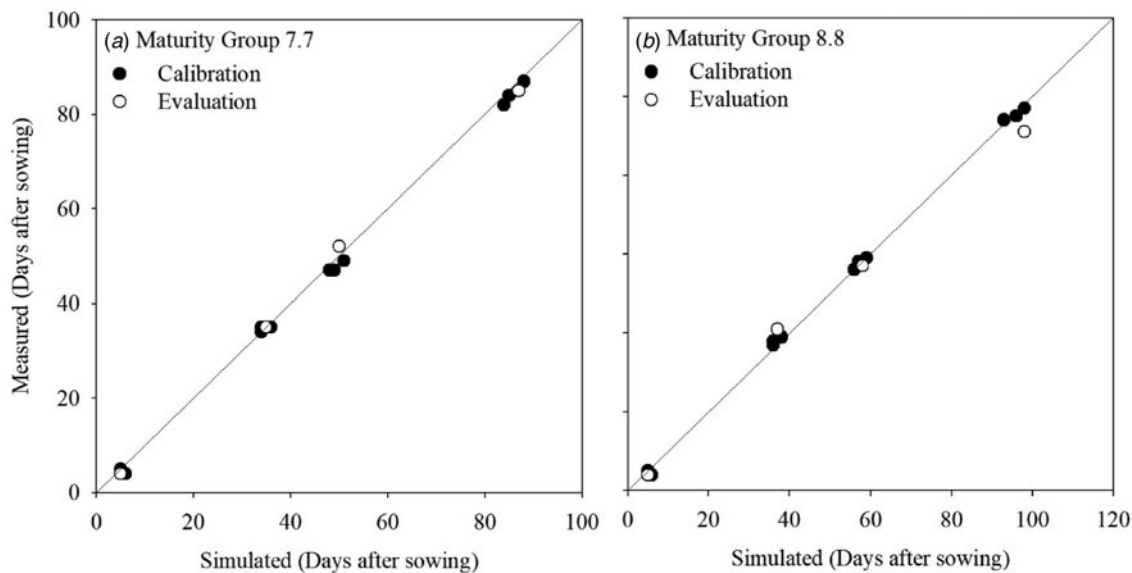


Fig. 3. Relationship between measured and simulated soybean crop stages (emergence, anthesis, first seed and maturity) for calibration and evaluation for maturity group 7.7 (a) and 8.8 (b). Absolute values and bias for calibration and evaluation steps can be found in Table 5.

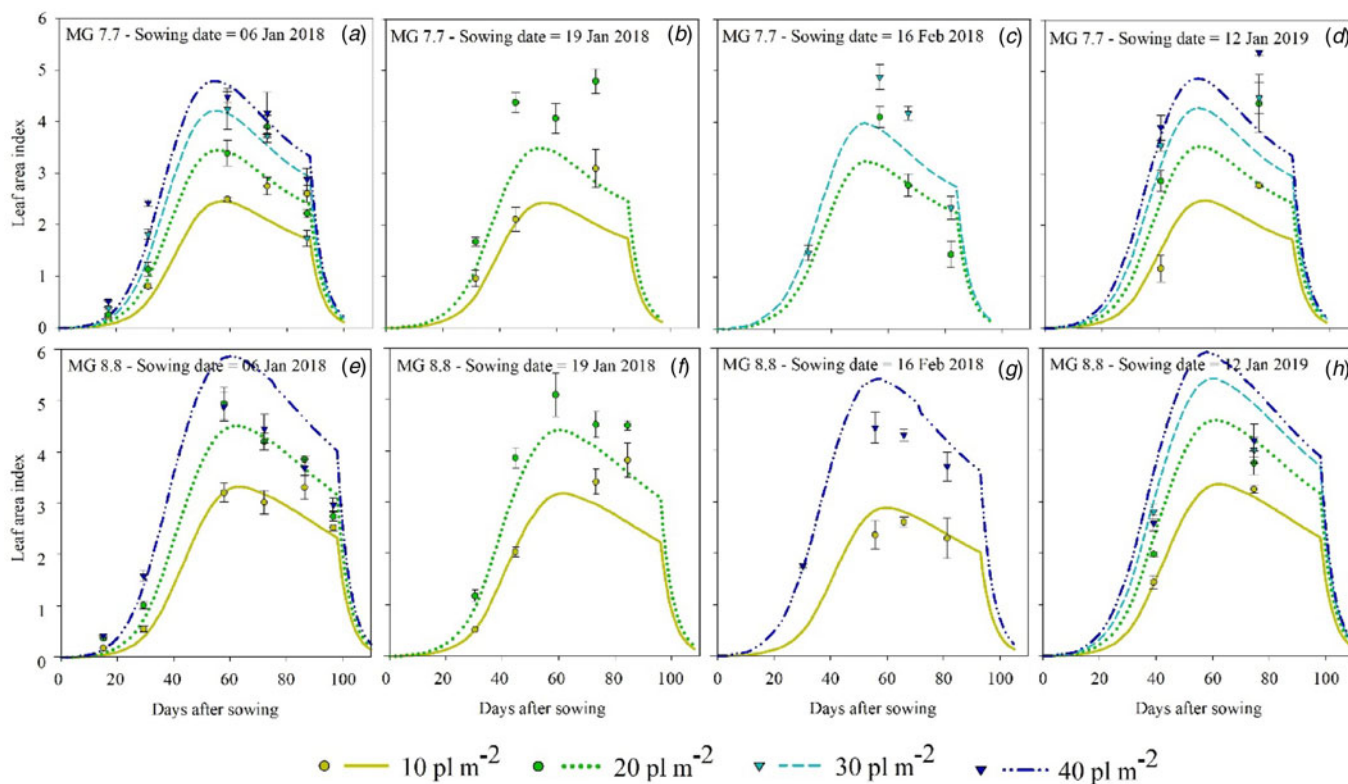


Fig. 4. (Colour online) Measured (symbols) and simulated (line) LAI over time for calibration (a, b, c, e, f and g) and evaluation (d and h) for MG 7.7 (a, b, c and d) and MG 8.8 (e, f, g and h) at four plant densities. Mean measured and simulated values, bias, RMSE and RRMSE can be found in Table S2 of the Supplementary material.

for all locations, sowing dates and maturity group (Fig. 7). However, the yield increase was greater when plant density was increased from 10 to 20 pl per m², followed by 20 to 30 pl per m² and 30 to 40 pl per m². The higher yield difference between plant density occurred for the sowing date on 21 Feb. and MG

8.8 in Santarém. Under this condition, median yields were 2658, 3197, 3442 and 3583 kg/ha (Fig. 7(f)), respectively, for 10, 20, 30 and 40 pl per m². The yield increase was 20, 8 and 4%, respectively, from 10 to 20, 20 to 30 and 30 to 40 pl per m². Porto Nacional had the lower response with plant density

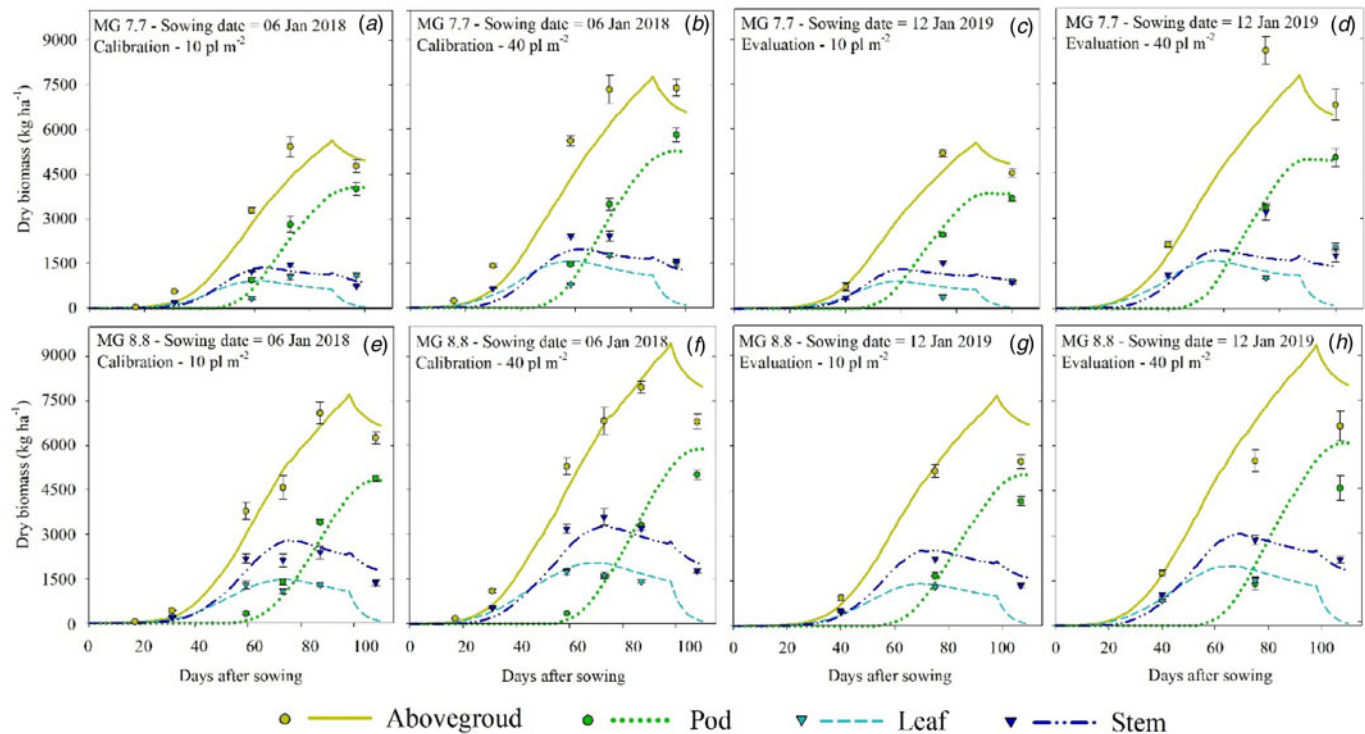


Fig. 5. (Colour online) Measured (symbols) and simulated (line) soybean above-ground biomass and partition to leaf, stem and pod over time for 10 pl per m² (a, c, e and g) and 40 pl per m² (b, d, f and h) sown on 06 Jan. 2018 (a, b, e and f) and 12 Jan. 2019 (c, d, g and h) for MG 7.7 (a, b, c and d) and 8.8 (e, f, g and h). Mean measured and simulated values, bias, RMSE and RRMSE can be found in Tables S3, S4, S5, S6 and S7 of the Supplementary material, respectively, for aboveground, leaf, pod and stem dry biomass.

increase for MG 8.8, from 1.2 to 7.3%, with a median yield across sowing dates of 2991, 3211, 3293 and 3332 kg/ha, respectively, for 10, 20, 30 and 40 pl per m² (Fig. 7(j)).

The yield across sowing dates had a similar response for MG 7.7 and 8.8 in Anapurus (Figs 7(a) and (b)), Paragominas (Figs 7(c) and (d)) and Santarém (Figs 7(e) and (f)). The greater inter-annual yield variability occurred at the beginning of the sowing window (01 Dec. and 11 Dec.), due to limiting weather conditions that can occur at the beginning of the sowing window. The delay of the sowing date increased the yield difference between plant densities in these sites. For example, the median yield for MG 7.7 with 40 pl per m² density was 635 kg/ha (25%) greater than that with 10 pl per m² for the 01 Dec. sowing date, and this yield difference between plant densities was 820 kg/ha (38%) for the 21 Feb. sowing date. For these three sites, the median yield typically reduced on delaying the sowing date, and the yield reduction with delayed sowing was larger for the lowest planting density than for the highest planting density. For example, the difference yield for MG 7.7 with 10 pl per m² sowing on 01 Dec. and 21 Feb. was 415 kg/ha, while this difference was 230 kg/ha for 40 pl per m².

The sowing dates resulted in two patterns of yield when considered MG 7.7 (Fig. 7(g)) and MG 8.8 (Fig. 7(h)) in Balsas. The two maturity groups showed very similar potential yield in the region, with, respectively, a mean yield of 3408 and 3335 kg/ha. MG 7.7 increased median yield, averaged across planting densities, from 3448 kg/ha on 01 Oct. to 3895 kg/ha on 11 Nov., reducing after that date until 21 Jan. In this scenario, the sowing date affects the yield difference between plant density, where early sowing date (01 Oct.) showed a mean difference between 10 and 40 pl per m² of 453 kg/ha, while late sowing (21 Jan.) reached a

difference of 662 kg/ha. However, MG 8.8 increased median yield, averaged across planting densities, from 3133 kg/ha on 01 Oct. to 3772 kg/ha on 21 Dec., reducing after data until 21 Jan.

Porto Nacional (Figs 7(i) and (j)) and Santana do Araguaia (Figs 7(k) and (l)) had similar yield levels and patterns across sowing dates, maturity groups and plant densities. MG 7.7 had a similar yield from 01 Oct. to 21 Nov., with a reduction until 21 Dec. for plant density of 20, 30 and 40 pl per m². However, plant density of 10 pl per m² showed a lower yield at the start and end of the sowing window, with the best sowing date occurring on 11 Nov., with a median yield of 3637 and 3591 kg/ha, respectively, for Porto Nacional (Fig. 7(i)) and Santana do Araguaia (Fig. 7(k)). The delay of sowing from 01 Oct. to 21 Dec. increased yield for MG 8.8, showing lower potential and yield difference between plant densities than MG 7.7 (Figs 7(j) and (l)).

Discussion

CSM-CROPGRO-Soybean demonstrated good performance for both MG 7.7 and 8.8 in response to plant densities and sowing dates in this short photoperiod low latitude environment. The performance of the model as described by statistical indices are similar to prior studies in Brazil for the north (Lima *et al.*, 2019), midwestern (Teixeira *et al.*, 2019) and southern (Battisti *et al.*, 2017) regions. Furthermore, a characteristic not accounted for by Grimm *et al.* (1993) in the default parameters is the presence of long juvenile phase introduced into soybean germplasm adapted to low latitude (Destro *et al.*, 2001; Carpentieri-Pipolo *et al.*, 2002; Sinclair *et al.*, 2005; Alliprandini *et al.*, 2009; Liu *et al.*, 2017). A value of 6 thermal days was added to the ecotype

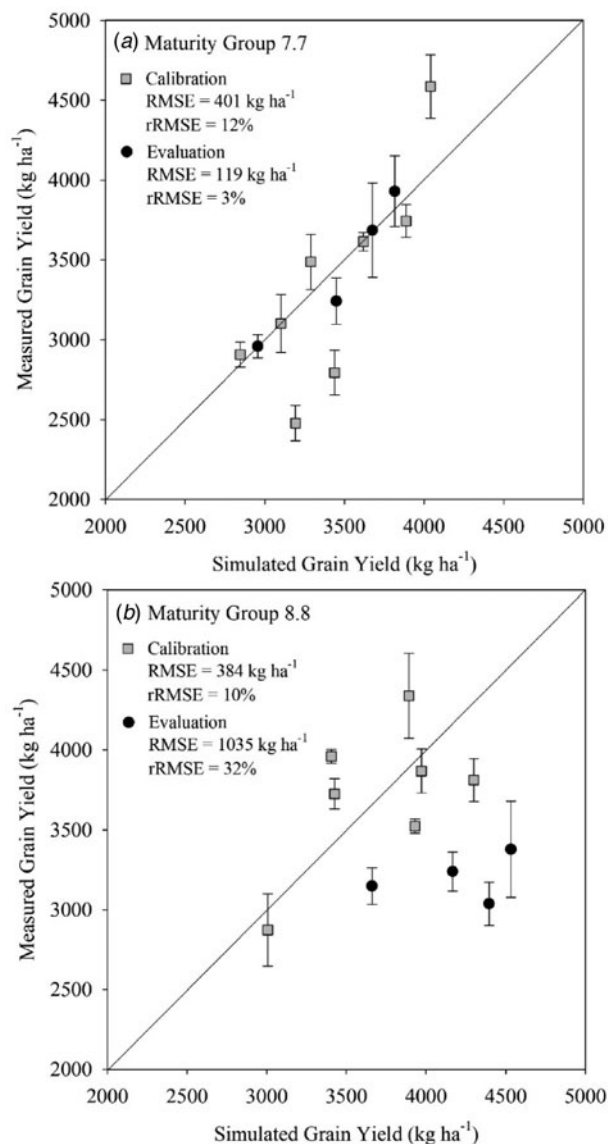


Fig. 6. Relation between simulated and measured soybean grain yield for calibration and evaluation for maturity group 7.7 (a) and 8.8 (b). RMSE is the root mean square error and RRMSE is the relative root mean square error.

parameter time required from first true leaf to end of the juvenile phase (V1-JU) (Table 4), which led to minimal effect of short photoperiod of this region on the time for first flower occurrence. However, this did not work as intended, therefore the effect of the juvenile trait was created by using a longer EM-FL parameter duration than the generic cultivar parameters presented by Boote *et al.* (2003).

The model had poorer phenology performance during the evaluation (2019 growing season) for MG 8.8. The crop model followed the same pattern for evaluation as for calibration, while the observed crop in the evaluation had a longer vegetative period (4-day delay of the first flower) and a shorter time from first flowering to beginning maturity (7 days earlier to beginning maturity). We hypothesize that this occurred because of an effect of water excess in the field associated with high cultivar sensitivity (Bajgain *et al.*, 2015; Pasley *et al.*, 2020). The crop model simulated a penalization for water excess lower than 1% (data not

shown). The potential water excess can be verified based on a high frequency of rainy days during the growing seasons (Figs 2 (b) and (c)), where the accumulated rainfalls were 1749 and 1928 mm from December to June, respectively, for 2017/18 and 2018/19 growing seasons.

CROPGRO-Soybean does simulate canopy height and width and does account for row spacing (Boote *et al.*, 1998) an approach required for its hedgerow light interception. Plant structure changes considerably across plant density due to soybean plasticity (Supplementary material, Fig. S2) (Carpenter *et al.*, 1997; Balbinot Junior *et al.*, 2018; Ferreira *et al.*, 2020). The plasticity increases branch number under low plant density in response to solar radiation interception, light quality and plant competition (Board, 2000; Nakano *et al.*, 2019). The leaf senescence was smaller in the field than in the crop model from the middle to the end of the cycle under low plant density (10 pl per m²). This may be associated with a less self-shading effect and a high number of branches, and high light may slow nitrogen mobilization from leaves, thus reducing leaf senescence (Boote and Pickering, 1994).

The interaction between maturity group, sowing dates and plant densities affected LAI dynamics and, consequently, potential yield. For example, MG 7.7 had LAI reaching value 3 later in the cycle (80 days after sowing) for 10 pl per m² (Figs 4(a), (b) and (d)), while plant densities above 20 pl per m² reached the LAI 3 value in less than 50 days after sowing.

A higher plant density typically increases aboveground biomass and LAI, but yield increase is conditioned by the cultivar adaptation to a given environment (Ball *et al.*, 2000; Board, 2000; Corassa *et al.*, 2018; Carciochi *et al.*, 2019). The crop model simulated well the yield, biomass and LAI for most cases across plant density and sowing dates. However, for MG 8.8 (determinate growth) sowing on 12 Jan. 2019 (Fig. 5(h)), the higher plant density did not result in an increase of yield at the field, while the crop model did increase yield in response to high plant density.

Seasonal analysis showed a higher soybean grain yield for a plant density of 40 pl per m², as expected (Fig. 7). However, a considerable yield increase occurred from 10 to 20 pl per m². This indicates that a minimum of plant density over 20 pl per m² is required for these sites (Fig. 7), ensuring soybean yield stability across sowing dates. The soybean plasticity across plant density is associated with adjustment in branch number, pod and seed number by area (Supplementary material, Fig. S2). The resultant effects include increased biomass partitioned to branches, the net photosynthesis, the efficiency of solar radiation interception by leaf area during the vegetative phase and the leaf expansion during reproductive phase (Carpenter and Board, 1997; Ball *et al.*, 2000; Board, 2000; Balbinot Junior *et al.*, 2018).

Plant density higher than 20 pl per m² showed higher yield, however, it is essential to consider cultivars resistance to lodging and the potential pressure of diseases in the region. These are conditions that can lead to yield losses when higher plant densities are used, and lodging and pests are not accounted for yield penalization by the crop model (Teixeira *et al.*, 2019). For example, Paragominas has a higher rainfall amount during the reproductive period when sowing occurs in January (Supplementary material, Fig. S1). High rainfall amount increases soybean rust pressure due to leaf wetness (Del Ponte *et al.*, 2006), where a plant density between 20 and 30 pl per m² has a preference to reach high potential yield and reduce diseases risk by lower leaf area (lower leaf wetness and more efficiency of application of chemical control).

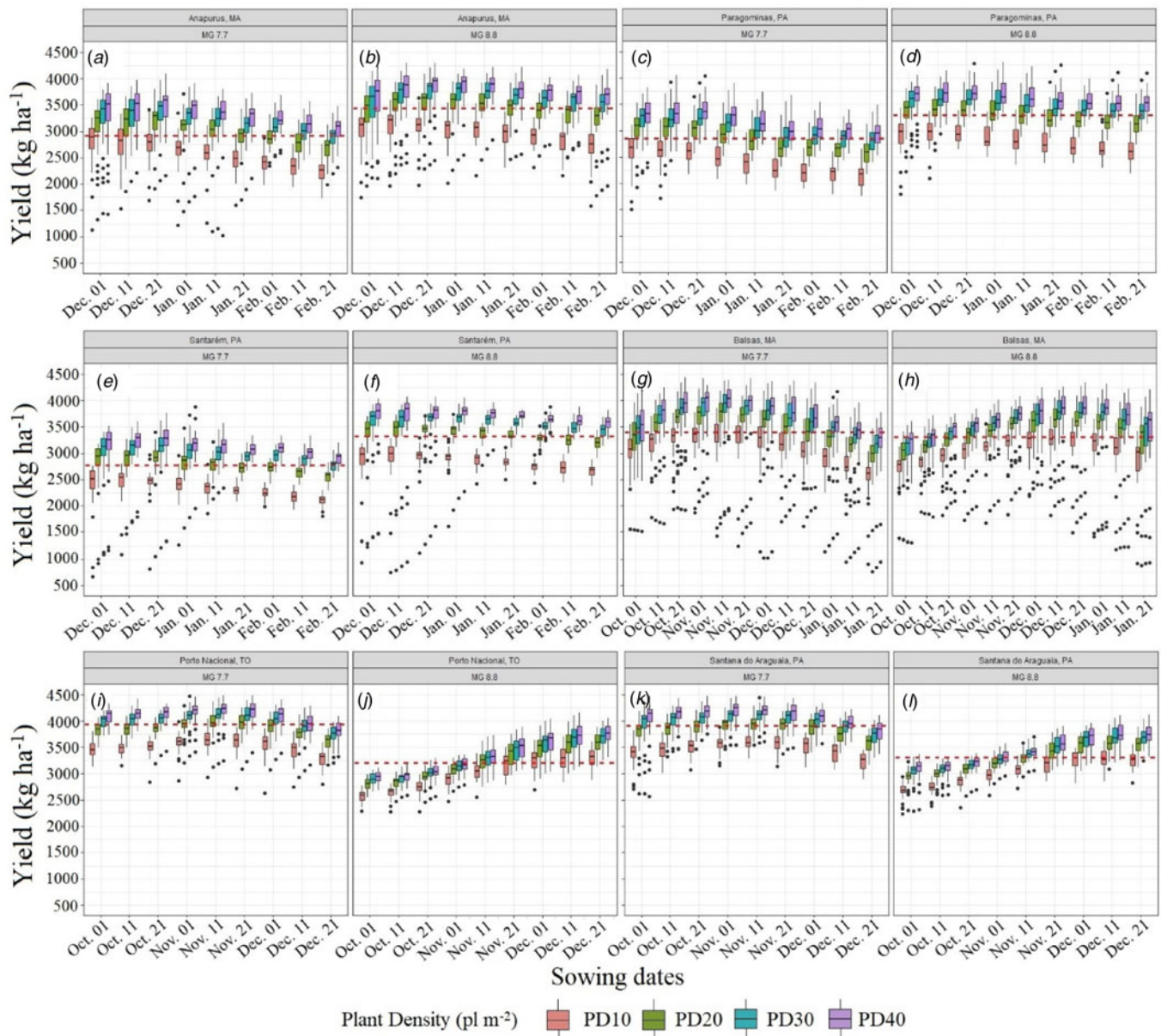


Fig. 7. (Colour online) Soybean grain yield simulated as a function of plant density (10 to 40 pl m^{-2}), sowing dates and maturity groups 7.7 (a, c, e, g, i and k) and 8.8 (b, d, f, h, j and l) across 33 growing seasons in Anapurus (a and b), Paragominas (c and d), Santarém (e and f), Balsas (g and h), Porto Nacional (i and j) and Santana do Araguaia (k and l). In the box-plot, the central line is the medium, the lower and upper hinges correspond to the first and third quartiles (the 25th and 75th percentiles), the upper and lower whisker extends from the hinge to the largest and smallest value, respectively, than $1.5 \times$ IQR from the hinge (where IQR is the inter-quartile range, or distance between the first and third quartiles), and data beyond the end of the whiskers are called 'outlying' points and are plotted individually. The red dashed line is the mean value across plant density and sowing date.

The maturity group and sowing dates affected the interaction between local weather and plant density over yield due to cycle duration and the time to achieve the optimum LAI for maximum light interception (Purcell *et al.*, 2002; Lee *et al.*, 2008; Zdziarski *et al.*, 2018). For the sites of low latitude, between 2° and 4° south, MG 8.8 had preference over MG 7.7 due to the higher average and stability yield across sowing window, while for sites below latitude 9° south, MG 7.7 had the preference of sowing. On the contrary, Balsas (latitude 8° south) had a similar average yield across sowing window for MG 7.7 and MG 8.8, but with the higher yield occurring for sowing dates, respectively, in November and December.

The maturity groups and sowing date patterns by location occurred due to cycle duration and potential yield associated with climate (Battisti and Sentelhas, 2019). The cycle duration defines the capacity of the crop to intercept solar radiation and, consequently, the potential yield (Van Roekel *et al.*, 2015). The longer cycle (MG 8.8) was a better strategy for low latitude, where water deficit is lower and longer cycle results in higher potential yield (Battisti and Sentelhas, 2019). The sites of higher latitude showed a preference for MG 7.7, mainly for early sowing dates. On the contrary, MG 8.8 had a higher yield for late sowing dates in Balsas, and a lower yield difference between MG 8.8 and MG 7.7 with early sowing dates in Porto Nacional and Santana do

Araguaia. This occurred due to the photoperiod reduction in late sowing dates accelerates the crop cycle of MG 7.7, resulting in less time for the crop to increase leaf area in low plant densities (Tagliapietra *et al.*, 2018).

Conclusion

CSM-CROPGRO-Soybean was able to simulate crop development and growth across maturity groups, sowing dates and plant densities in the short-day low latitude environment. Multi-year seasonal analysis indicated that plant density of 40 pl per m² leads to higher yield in all sites, sowing dates and maturity groups simulated in the crop model. However, high plant density can lead to yield losses by plant lodging and increase disease pressure by higher leaf area, increasing leaf wetness and reducing the efficiency of application of chemical control. Lodging and diseases are factors that crop models are not accounted for in yield simulation. Overall, the 20 pl per m² is a minimum plant density required for soybean production in this region, due to the higher yield increase that occurred when plant density was increased from 10 to 20 pl per m², leading to high yield gain and relive to lower seed costs. Further to plant density, the planning of maturity groups and sowing dates by sites showed to be important factors by the different response patterns, which can help to improve soybean yield.

Supplementary material. The supplementary material for this article can be found at <https://doi.org/10.1017/S0021859621000204>.

Acknowledgements. The authors would like to thank the Juparaná Agrícola farm for field support; the Universidade Federal de Santa Catarina for the post-doc position for the first author in the Postgraduate Program in Agroecosystems, especially for the contribution from Prof. Dr S. L. Schindwein.

Financial support. Support for the second author from the National Council for Scientific and Technological Development (CNPq) through Financial Support to Research (Process No. 405740/2018-2) is gratefully acknowledged.

Conflict of interest. None.

References

- Alliprandini LF, Abatti C, Bertagnoli PF, Cavassim JE, Gabe HL, Kurek A, Marsumoto MN, Oliveira MAR, Pitol C, Prado LC and Steckling C (2009) Understanding soybean maturity groups in Brazil: environment, cultivar classification, and stability. *Crop Science* **49**, 801–808.
- Alvares CA, Stape JL, Sentelhas PC, Gonçalves JLM and Sparovek G (2013) Köppen's climate classification map for Brazil. *Meteorologische Zeitschrift* **22**, 711–728.
- Bajgain R, Kawasaki Y, Akamatsu Y, Tanaka Y, Kawamura H, Katsura K and Shiraiwa T (2015) Biomass production and yield of soybean grown under converted paddy fields with excess water during the early growth stage. *Field Crops Research* **180**, 221–227.
- Balbinot Junior AA, de Oliveira MCN, Zucareli C, Ferreira AS, Werner F and Silva MAA (2018) Analysis of phenotypic plasticity in indeterminate soybean cultivars under different row spacing. *Australian Journal of Crop Science* **12**, 648–654.
- Ball RA, Purcell LC and Vories ED (2000) Optimizing soybean plant population for a short-season production system in the southern USA. *Crop Science* **40**, 757–764.
- Banternig P, Hoogenboom G, Patanothai A, Singh P, Wani SP, Pathak P, Tongpoon-pol S, Atichart S, Srihaban P, Buranaviriyakul S, Jintrawet A and Nguyen TC (2009) Application of the cropping system model (CSM)-CROPGRO-soybean for determining optimum management strategies for soybean in tropical environments. *Journal of Agronomy and Crop Science* **196**, 231–242.
- Basso B, Ritchie JT, Pierce JE, Braga RP and Jones JW (2001) Spatial validation of crop models for precision agriculture. *Agricultural Systems* **68**, 97–112.
- Battisti R and Sentelhas PC (2019) Characterizing Brazilian soybean-growing regions by water deficit patterns. *Field Crop Research* **240**, 95–105.
- Battisti R, Sentelhas PC and Boote KJ (2017) Inter-comparison of performance of soybean crop simulation models and their ensemble in southern Brazil. *Field Crops Research* **200**, 28–37.
- Battisti R, Sentelhas PC, Parker PS, Nendel C, Câmara GMS, Farias JRB and Basso CJ (2018) Assessment of crop-management strategies to improve soybean resilience to climate change in Southern Brazil. *Crop and Pasture Science* **69**, 154–162.
- Battisti R, Ferreira MDP, Tavares ÉB, Knapp FM, Bender FD, Casaroli D and Alves Júnior J (2020a) Rules for grown soybean-maize cropping system in midwestern Brazil: food production and economic profits. *Agricultural Systems* **182**, 102850.
- Battisti R, Casaroli D, Paixão JS, Alves Júnior J, Evangelista AWP and Mesquita M (2020b) Assessment of soybeans crop management strategies using crop growth models for central Brazil. In Mirschel W, Terleev V and Wenkel KO (eds), *Landscape Modelling and Decision Support*. Cham, Switzerland: Springer, pp. 525–543. doi:10.1007/978-3-030-37421-1_27.
- Board JE (2000) Light interception efficiency and light quality affect yield compensation of soybean at low plant populations. *Crop Science* **40**, 1285–1294.
- Boote KJ and Pickering NB (1994) Modeling photosynthesis of row crop canopies. *HortScience* **29**, 1423–1434.
- Boote KJ, Jones JW, Hoogenboom G and Pickering NB (1998) Simulation of crop growth: CROPGRO model. In Peart RM and Curry RB (eds), *Agricultural Systems Modeling and Simulation*. New York: Marcel Dekker, pp. 651–692.
- Boote KJ, Jones JW, Batchelor WD, Nafziger ED and Myers O (2003) Genetic coefficients in the CROPGRO-soybean model. *Agronomy Journal* **95**, 32–51.
- Boote KJ, Jones JW, White JW, Asseng S and Lizaso JI (2013) Putting mechanisms into crop production models. *Plant, Cell and Environment* **36**, 1658–1672.
- Carciochi WD, Schwalbert R, Andrade FH, Corassa GM, Carter P, Gaspar AP, Schmidt J and Ciampitti IA (2019) Soybean seed yield response to plant density by yield environment in North America. *Agronomy Journal* **111**, 1923–1932.
- Carpenter AC and Board JE (1997) Branch yield components controlling soybean yield stability across plant populations. *Crop Science* **37**, 885–891.
- Carpentieri-Pípolo V, de Almeida LA and de Kiihl RAS (2002) Inheritance of a long juvenile period under short-day conditions in soybean. *Genetics and Molecular Biology* **25**, 463–469.
- Cattelan AJ and Dall'Agnol A (2018) The rapid soybean growth in Brazil. *Oilseeds and Fats Crops and Lipids* **25**, 1–12.
- CONAB (2020) Crops historical data. Available at: <https://www.conab.gov.br/info-agro/safras/>. Accessed 02 March 2020 (in Portuguese).
- Corassa GM, Amado TJC, Strieder ML, Schwalbert R, Pires JLF, Carter PR and Ciampitti IA (2018) Optimum soybean seeding rates by yield environment in southern Brazil. *Agronomy Journal* **110**, 2430–2438.
- Del Ponte EM, Godoy CV, Li X and Yang XB (2006) Predicting severity of Asian soybean rust epidemics with empirical rainfall models. *Phytopathology* **96**, 797–803.
- Destro D, Afonso R, Kiihl DS, Alves L and Almeida D (2001) Photoperiodism and genetic control of the long juvenile period in soybean. *Crop Breeding and Applied Biotechnology* **1**, 72–92.
- Ewert F, Rötter RP, Bindi M, Webber H, Trnka M, Kersebaum KC, Olesen JE, van Ittersum MK, Janssen S, Rivington M, Semenov MA, Wallach D, Porter JR, Stewart D, Verhagen J, Gaiser T, Palosuo T, Tao F, Nendel C, Roggero PP, Bartosová L and Asseng S (2015) Crop modelling for integrated assessment of risk to food production from climate change. *Environmental Modelling & Software* **72**, 287–303.
- FAOSTAT (2020) Food and agriculture data. Available at: <http://www.fao.org/faostat/en/#home>. Accessed 15 February 2020.
- Ferreira AS, Zucareli C, Fonseca ICB and Balbinot Junior AA (2020) Minimum optimal seeding rate for indeterminate soybean cultivars grown in tropics. *Agronomy Journal* **112**, 2092–2102.

- Grimm SS, Jones JW, Boote KJ and Hesketh JD (1993) Parameter estimation for predicting flowering date of soybean cultivars. *Crop Science* **33**, 137–144.
- Halsnaes K and Taerup S (2009) Development and climate change: a mainstreaming approach for assessing economic, social, and environmental impacts of adaptation measures. *Environmental Management* **43**, 765–778.
- Hoogenboom G, Porter CH, Shelia V, Boote KJ, Singh U, White JW, Hunt LA, Ogoshi R, Lizaso JI, Koo J, Asseng S, Singels A, Moreno LP and Jones JW (2017) *Decision Support System for Agrotechnology Transfer (DSSAT) Version 4.7.0.0*. Gainesville, Florida, USA: DSSAT Foundation. <https://DSSAT.net>
- Hoogenboom G, Porter CH, Boote KJ, Shelia V, Wilkens PW, Singh U, White JW, Asseng S, Lizaso JI, Moreno LP, Pavan W, Ogoshi R, Hunt LA, Tsuji GY and Jones JW (2019) The DSSAT crop modeling ecosystem. In Boote KJ (ed.), *Advances in Crop Modeling for a Sustainable Agriculture*. Cambridge, United Kingdom: Burleigh Dodds Science Publishing, pp. 173–216.
- Hu M and Wiatrak P (2012) Effect of planting date on soybean growth, yield, and grain quality: review. *Agronomy Journal* **104**, 785–790.
- Hunt LA and Boote KJ (1998) Data for model operation, calibration, and evaluation. In Tsuji GY, Hoogenboom G and Thornton PK (eds), *Understanding Options for Agricultural Production*. Dordrecht: Springer, pp. 9–39.
- IBGE (National Institute of Geography and Statistics) (2020) Agricultural Production. In Portuguese. Available at <http://www.sidra.ibge.gov.br/bda/pesquisas/pam>. Accessed 12 April 2020 (in Portuguese).
- Jones JW, Jianqiang H, Boote KJ, Wilkens P, Porter CH and Hu Z (2011) Estimating DSSAT cropping system cultivar-specific parameters using Bayesian techniques. In Ahuja LR and Ma L (eds). *Methods of Introducing System Models Into Agricultural Research*. Madison: ASA; CSSA; SSSA, pp. 365–394, 2011. (Advances in Agricultural Systems Modeling, 2).
- Justino LF, Alves Júnior J, Battisti R, Heinemann AB, Leite CV, Evangelista AWP and Casaroli D (2019) Assessment of economic returns by using a central pivot system to irrigate common beans during the rainfed season in Central Brazil. *Agricultural Water Management* **224**, 104749.
- Lee CD, Egli DB and TeKrony DM (2008) Soybean response to plant population at early and late planting dates in the Mid-South. *Agronomy Journal* **100**, 971–976.
- Lima MJA, Oliveira EC, Sampaio LS, William FC and Souza PJOP (2019) Agrometeorological analysis of the soybean potentiality in an Amazonian environment. *Pesquisa Agropecuária Tropical* **49**, 1–9.
- Liu X, Wu JA, Ren H, Qi Y, Li C, Cao J, Zhang X, Zhang Z, Cai Z and Gai J (2017) Genetic variation of world soybean maturity date and geographic distribution of maturity groups. *Breeding Science* **67**, 221–232.
- Makowski D, Wallach D and Tremblay M (2002) Using Bayesian approach to parameter estimation: comparison of the GLUE and MCMC methods. *Agronomie* **22**, 191–203.
- MAPA (Minister of Agriculture, Livestock and Food Supply) (2020) Agroclimatic Risk Zoning. Available from: <http://www.agricultura.gov.br/politica-agricola/zoneamento-agricola>. Accessed: 01 December 2020.
- Nakano S, Purcell LC, Homma K and Shiraiwa T (2019) Modeling leaf area development in soybean (*Glycine max* L.) based on the branch growth and leaf elongation. *Plant Production Science* **22**, 1–13.
- Nendel C, Berg M, Kersebaum KC, Mirschel W, Specka X, Wegehenkel M, Wendel KO and Wieland R (2011) The MONICA model: testing predictability for crop growth, soil moisture and nitrogen dynamics. *Ecological Modelling* **222**, 1614–1624.
- Nóia Junior RS and Sentelhas PC (2019) Soybean-maize succession in Brazil: impacts of sowing dates on climate variability, yields and economic profitability. *European Journal of Agronomy* **103**, 140–151.
- Pasley HR, Huber I, Castellano MJ and Archontoulis SV (2020) Modeling flood-induced stress in soybeans. *Frontiers in Plant Science* **11**, 1–13.
- Purcell LC, Ball RA, Reaper JD and Vories ED (2002) Radiation use efficiency and biomass production in soybean at different plant population densities. *Crop Science* **42**, 172–177.
- RADAMBRASIL (1974) Survey of natural resources. Vol. 4. (In Portuguese.) Brazilian Gov., Ministry of Mines and Energy, Rio de Janeiro.
- Salmerón M, Purcell LC, Vories ED and Shannon G (2017) Simulation of genotype-by-environment interactions on irrigated soybean yields in the U.S. Midsouth. *Agricultural Systems* **150**, 120–129.
- Salmerón M, Gbur EE, Bourland FM, Earnest L, Golden BR and Purcell LC (2015) Soybean maturity group choices for maximizing radiation interception across planting dates in the Midsouth United States. *Agronomy Journal* **107**, 2132–2142.
- Setiyono TD, Cassman KG, Specht JE, Dobermann A, Weiss A, Yang H, Conley SP, Robinson AP, Pedersen P and De Bruin JL (2010) Simulation of soybean growth and yield in near-optimal growth conditions. *Field Crop Research* **119**, 161–174.
- Silva EHF, Pereira RAA, Gonçalves AO, Bordignon ÁZ and Marin FR (2017) Simulation of soybean yield in Piracicaba-SP based on climate change. *Agrometeoros* **25**, 9–17.
- Sinclair TR, Neumaier N, Farias JRB and Nepomuceno AL (2005) Comparison of vegetative development in soybean cultivars for low-latitude environments. *Field Crops Research* **92**, 53–59.
- Spehar CR, Francisco ER and Pereira EA (2015) Yield stability of soybean cultivars in response to sowing date in the lower latitude Brazilian Savannah Highlands. *Journal of Agricultural Science* **153**, 1059–1068.
- Tagliapietra EL, Streck NA, da Rocha TSM, Richter GL, da Silva MR, Cera JC and Junior Zanon A (2018) Optimum leaf area index to reach soybean yield potential in subtropical environment. *Agronomy Journal* **110**, 932–938.
- Teixeira WWR, Battisti R, Sentelhas PC, de Moraes MF and de Oliveira Junior A (2019) Uncertainty assessment of soya bean yield gaps using DSSAT-CSM-CROPGRO-soybean calibrated by cultivar maturity groups. *Journal of Agronomy and Crop Science* **205**, 1–12.
- Van Roekel RJ, Purcell LC and Salmerón M (2015) Physiological and management factors contributing to soybean potential yield. *Field Crops Research* **182**, 86–97.
- Wallach D, Makowski D and Jones JW (2006) *Working with Dynamic Crop Models: Evaluation, Analysis, Parameterization and Applications*. Amsterdam: Elsevier, pp. 1–462.
- Xavier AC, King CW and Scanlon BR (2015) Daily gridded meteorological variables in Brazil (1980–2013). *International Journal of Climatology* **36**, 2644–2659.
- Zdziarski AD, Todeschini MH, Milioli AS, Woyann LG, Madureira A, Stoco MG and Benin G (2018) Key soybean maturity groups to increase grain yield in Brazil. *Crop Science* **58**, 1155–1165.